NANO LETTERS

Letter

pubs.acs.org/NanoLett

A Transmission Electron Microscopy Study of the Electrochemical Process of Lithium−Oxygen Cells

Hun-Gi Jung,[†] Hee-Soo Kim,[‡] Jin-Bum Park,[†] In-Hwan Oh,[§] Jusef Hassoun,[⊥] Chong Seung Yoon,*[,‡] Bruno Scrosati,*[,†,⊥] and Yang-Kook Sun*[,†,∥]

[†]Department of WCU Energy Engineering and [‡]Department of Materials Science and Engineering, Hanyang University, Seoul 133-791, South Korea

[§]Fuel Cell Center, Korea Institute of Science and Technology, Seoul 136-791, South Korea

[⊥]Department of Chemistry, University of Rome Sapienza, 00185, Rome, Italy

[∥]Department of Chemical Engineering, Hanyang University, Seoul 133-791, South Korea

Supporting Information

ABSTRACT: The electrochemical reaction of a lithium−oxygen cell using a tetraethylene glycol dimethyl ether-lithium triflate, TEGDME-$LiCF_3SO_3$ electrolyte, is investigated by a detailed transmission electron microscopy analysis. The results confirm the reversibility of the process by showing the formation−dissolution of lithium peroxide, Li_2O_2, upon repeating cell charge and discharge cycles.

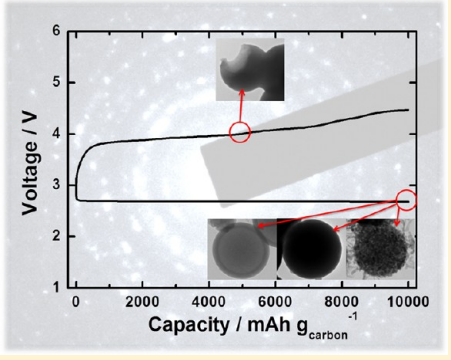

KEYWORDS: *Lithium−oxygen cell, transmission electron microscopy, electrochemical reaction, reversible charge−discharge process, rechargeable lithium−air battery*

Lithium−oxygen batteries have recently received a great deal of attention due to the value of their energy density, the highest among all other existing electrochemical power sources.[1−5] The basic cell reaction: $2Li + O_2 \leftrightarrows Li_2O_2$, gives a theoretical energy density of the order of 3500 Wh kg^{-1} considering the Li_2O_2 mass. However, many issues associated with both electrodes and electrolyte still prevent the practical achievement of this outstanding energy value. Conventional lithium battery electrolytes, such as those based on organic carbonate solutions used in the initial development of Li−air batteries,[4−7] are not appropriate since they are readily attacked by the nucleophilic species associated with the oxygen electrochemical process.[5,6,8] Consequently, the identification of a stable electrolyte capable of allowing extended electrochemical cycling is still a major challenge in the Li−air battery technology. We have recently shown[9] that a solution of lithium triflate, $LiCF_3SO_3$ in tetraethylene glycol dimethyl ether (TEGDME)-$LiCF_3SO_3$, is a promising candidate.[1,3] We have exploited this electrolyte for assembling stable lithium−oxygen cells in order to investigate and clarify the lithium−oxygen electrochemical process by carrying out a unique study based on a detailed transmission electron microscopy (TEM) analysis. To our knowledge, this particular analytic approach to investigate the electrochemical behavior of lithium−oxygen cells is quite innovative.

Figure 1 shows the discharge (oxygen reduction)−charge (oxygen evolution) voltage profiles of a Li−O_2, coin-type cell

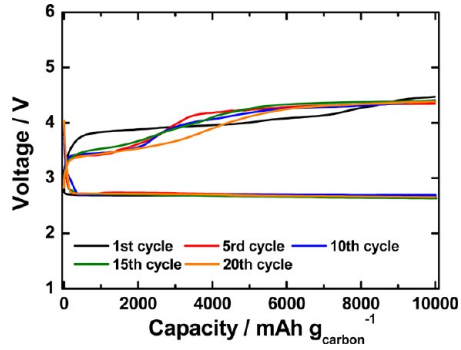

Figure 1. Discharge (oxygen reduction to Li_2O_2)−charge (Li_2O_2 reconversion in oxygen and lithium) cycles of a lithium−oxygen cell at room temperature. Galvanostatic, time-controlled mode. Current: 500 mA g_{carbon}^{-1} (0.5 mA cm^{-2} current, 1 mg cm^{-2} carbon loading). Time: 20 h. Cycling capacity: 10 000 mAh g_{carbon}^{-1}.

Received: May 31, 2012
Revised: July 17, 2012
Published: July 19, 2012

using a $LiCF_3SO_3$-TEGDME electrolyte and a porous, catalyst-free, Super P cathode (see Supporting Information for more details), cycled under capacity-controlled conditions for 20 times. Following an activation process, likely associated with an initial, nonuniform oxygen distribution throughout the oxygen electrode substrate, the cell assumed a steady response with a relatively small polarization gap between discharge (~2.8 V) and charge (~4.3 V) voltages. It should be noted that the cycling test was performed under the fixed capacity regime of 10 000 mAh g_{carbon}^{-1} (0.5 mA cm^{-2} current, 1 mg cm^{-2} carbon loading). The reproducibility of the charge−discharge voltage profiles under this very high capacity level (to our knowledge never obtained so far for Li−O_2 cells) suggests a high reversibility of the Li_2O_2 formation−dissolution process, as also confirmed by X-ray diffraction (XRD) analysis run on the Super P cathode before and after charging at the first, fifth and tenth cycle: lithium peroxide, Li_2O_2, was in fact detected as the main product after all discharges while no traces of it were observed in the following charges, see Figure S1 in the Supporting Information.

The Li_2O_2 discharge product is metastable and its presence in Li−O_2 cells has been investigated in the past by microspectroscopy, however, mostly limited to scanning electron microscopy (SEM) analyses.[7,10−12] Using our cell, which benefits from a stable TEGDME electrolyte we have been able to carry out a unique, detailed TEM analysis that has allowed us to closely track the morphological evolution of the cell reaction products at different stages of the discharge/charge cycles. Numerous spherical Li_2O_2 particles, whose sizes are in the range of several hundreds of nanometers, were routinely observed on the oxygen electrode discharged to 5000 mAh g_{carbon}^{-1} (see TEM images of Figure 2a,b). As expected, when the discharge was extended to 10 000 mAh g_{carbon}^{-1}, the particles grew in size (see images of Figure 2c,d).

Quite interestingly, the morphology of the Li_2O_2 particles varies on the surface of the discharged electrode. Figure 3 shows TEM images taken in different parts of the same sample after discharge at 10 000 mAh g_{carbon}^{-1} fixed capacity regime. The image of Figure 3a reveals a morphology characterized by a mixture of solid Li_2O_2 particles combined with perfect spherical hollow particles having wall thickness of about 50 nm. The hollow particles were amorphous as confirmed by the electron diffraction pattern shown in the inset of Figure 3a. The amorphous structure with no structural anisotropy accounts for the spherical morphology of the discharge product. However, crystalline Li_2O_2 nanoparticles were also found on the solid particle surface of the same electrode (see image in Figure 3c that shows a Li_2O_2 particle covered by 10 nm size crystalline primary nanoparticles). The polycrystalline electron diffraction pattern in the inset was indexed to hexagonal Li_2O_2 structure (see also Supporting Information Figure S2). The high-resolution TEM image shown in Figure 3d confirms the crystalline nature of the Li_2O_2 particles (see also Supporting Information Figure S3). At the present, we have no definitive model to account for these structural differences because there are many parameters that can influence the morphology of the electrodeposited Li_2O_2 particles, including a nonuniform distribution of the current over the carbon electrode surface, changes in nucleation rate, and so forth. We can tentatively assume that during the initial stage of the process the discharge product is predominantly formed by amorphous, spherical Li_2O_2 particles while crystalline Li_2O_2 primary particles start to nucleate on the preexistent amorphous particle surface toward

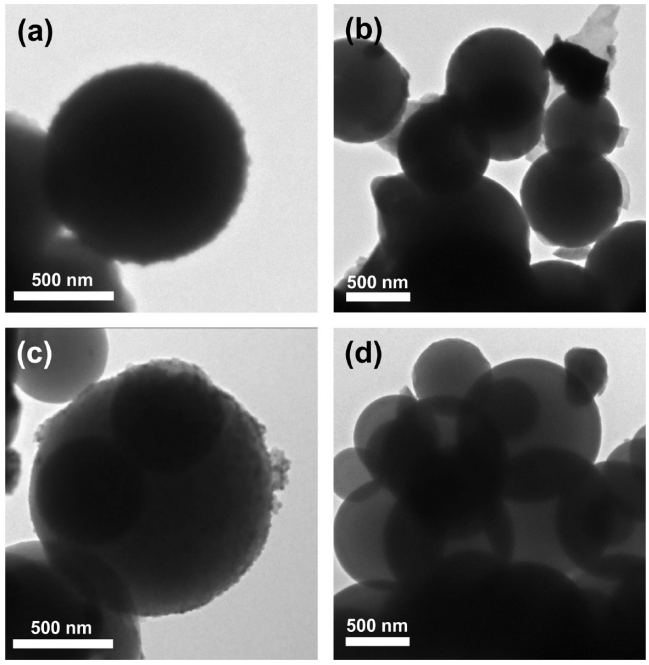

Figure 2. TEM images of the oxygen electrode at different discharged states. Images (a,b) refer to the oxygen electrode discharged at a fixed capacity of 5000 mAh g_{carbon}^{-1} (0.5 mA cm^{-2} current, 1 mg cm^{-2} carbon loading). Images (c,d) of the same electrode after discharge at a fixed capacity of 10 000 mAh g_{carbon}^{-1}.

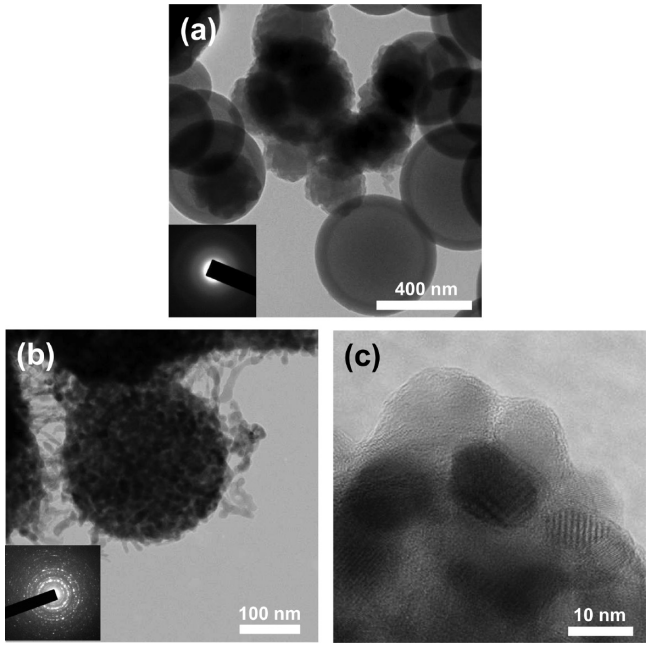

Figure 3. TEM images of different parts of the oxygen electrode discharged at 10 000 mAh g_{carbon}^{-1} (0.5 mA cm^{-2} current, 1 mg cm^{-2} carbon loading). Image (a) shows the electrode morphology characterized by a mixture of amorphous solid Li_2O_2 particles combined with perfect spherical hollow particles having wall thickness of about 50 nm. Image (b) shows a Li_2O_2 particle covered by 10 nm size crystalline primary nanoparticles. Inset images of (a,b) show selected area electron diffraction patterns of the particles; the high-resolution TEM image (c) shows the crystalline nature of the primary particles.

dx.doi.org/10.1021/nl302066d | Nano Lett. 2012, 12, 4333−4335

the end of the discharge, as also confirmed by the XRD spectra taken as a function of the state of discharge and reported in Supporting Information Figure S4.

A plausible route for formation of hollow spherical structures in the oxygen electrode of the Li−O_2 cell is the building-up of Li_2O_2 layers in the oxygen-rich environment on the particle surface during discharge and the concurrent decomposition of metastable Li_2O_2 in the oxygen-poor core. The simultaneous formation on the outer surface and decomposition on the inner surface would in fact allow the hollow structure to expand while maintaining the shell thickness. It is speculated that pressure build-up inside the hollow particles can also cause particle rupture, as for the examples shown in Supporting Information Figure S5a. These broken particles appear similar in appearance to the "doughnut"-shaped Li_2O_2 particles often imaged with SEM.[11,12] In addition to the hollow particles, both solid and collapsed particles were found among the discharge product, see Supporting Information Figure S5b.

The TEM analysis thus provides the means for attempting to shed light on the so far not yet totally clarified electrochemical process of the lithium−oxygen cell. TEM images taken on the discharged oxygen electrode at the fifth and tenth cycle of a cell cycled at the limited capacity of 10 000 mAh g_{carbon}^{-1} (0.5 mA cm^{-2} current, 1 mg cm^{-2} carbon loading) showed that the morphology of the Li_2O_2 solid particles is preserved upon cycling, see Figure 4a, this providing a first, convincing evidence

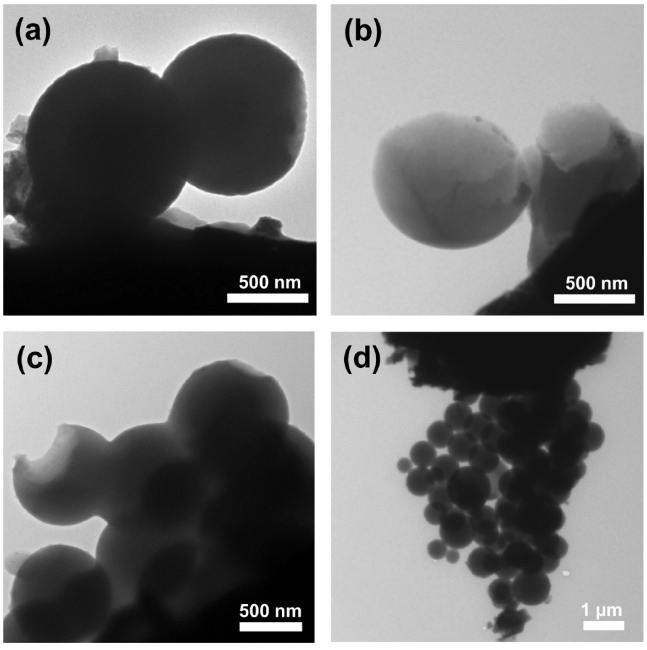

Figure 4. TEM images of Li_2O_2 particles in a lithium−oxygen cell fully discharged at a capacity of 10 000 mAh g_{carbon}^{-1} (a) and after a partial recharge up to a capacity of 5000 mAh g_{carbon}^{-1} (b−d). The images of the recharged cell reveal the progressive dissolution of the Li_2O_2 particles showing clear evidence of morphological changes such as cracking and reduction in diameter.

of the reversibility of the electrochemical process. The TEM analysis was then extended to the entire charge−discharge cycle. The images show that by passing from a fully discharged state to a partial recharge up to 5,000 mAh g_{carbon}^{-1} (0.5 mA cm^{-2} current, 1 mg cm^{-2} carbon loading), the Li_2O_2 particles started to dissolve, as clearly evidenced by the solid particle surface in Figure 4b and the cracked hemispherical hollow particles in Figure 4c. The progressive decrease in diameter of the Li_2O_2 hollow spherical particles and their partial dissolution upon cycling, see Figure 4d, furnish further evidence for the reversibility of the lithium−oxygen cell.

In conclusion, the TEM data reported here demonstrate the full reversibility of the oxygen electrochemical reaction in a lithium cell, confirming the results already obtained in our laboratory by scanning electron microscopy and secondary ion mass spectrometry studies.[9] We believe that the results reported in this work provide a step forward in the understanding of the lithium−oxygen cell electrochemistry, hence that they are of strong relevance for the progress of the lithium−air battery technology.

Details on the techniques used as well as on the structure of the experimental cell used in this work are reported in the Supporting Information.

■ ASSOCIATED CONTENT

Ⓢ Supporting Information

Experimental procedures, additional TEM images, and XRD data. This material is available free of charge via the Internet at http://pubs.acs.org.

■ AUTHOR INFORMATION

Corresponding Author

*E-mail: (Y.-K.S.) yksun@hanyang.ac.kr; (B.S.) bruno.scrosati@uniroma1.it; (C.S.Y.) csyoon@hanyang.ac.kr.

Notes

The authors declare no competing financial interest.

■ ACKNOWLEDGMENTS

This work was supported by the Human Resources Development of the Korea Institute of Energy Technology Evaluation and Planning (KETEP) grant funded by the Korea government Ministry of Knowledge Economy (No. 20114010203150) and by the SEED Project "REALIST" supported by the Italian Institute of Technology, IIT.

■ REFERENCES

(1) Laoire, C. Ó.; Mukerjee, S.; Abraham, K. M.; Plichta, E. J.; Hendrickson, M. A. *J. Phys. Chem. C* **2010**, *114*, 9178−9186.
(2) Hassoun, J.; Croce, F.; Armand, M.; Scrosati, B. *Angew. Chem., Int. Ed.* **2011**, *50*, 2999−3002.
(3) Laoire, C. Ó.; Mukerjee, S.; Plichta, E. J.; Hendrickson, M. A.; Abraham, K. M. *J. Electrochem. Soc.* **2011**, *158*, A302−A308.
(4) Ogasawara, T.; Debart, A.; Holzapfel, M.; Novak, P.; Bruce, P. G. *J. Am. Chem. Soc.* **2006**, *128*, 1390−1393.
(5) Freunberger, S. A.; Chen, Y.; Peng, Z.; Griffin, J. M.; Hardwick, L. J.; Bardé, F.; Novák, P.; Bruce, P. G. *J. Am. Chem. Soc.* **2011**, *133*, 8040−8047.
(6) Mizuno, F.; Nakanishi, S.; Kotani, Y.; Yokoishi, S.; Iba, H. *Electrochemistry* **2010**, *78*, 403−405.
(7) Debart, A.; Peterson, A. J.; Bao, J.; Bruce, P. G. *Angew. Chem., Int. Ed.* **2008**, *47*, 4521−4524.
(8) McCloskey, B. D.; Bethune, D. S.; Shelby, R. M.; Girishkumar, G.; Luntz, A. C. *J. Phys. Chem. Lett.* **2011**, *2*, 1161−1166.
(9) Jung, H.-G.; Hassoun, J.; Park, J.-B.; Sun, Y.-K.; Scrosati, B. *Nature Chem.* **2012**, *4*, 579−586.
(10) Lu, Y.-C.; Kwabi, D. G.; Yao, K. P. C.; Harding, J. R.; Zhou, J.; Zuind, L.; Shao-Horn, Y. *Energy Environ. Sci.* **2011**, *4*, 2999−3007.
(11) Mitchell, R. R.; Gallant, B. M.; Thompson, C. V.; Shao-Horn, Y. *Energy Environ. Sci.* **2011**, *4*, 2952−2958.
(12) Black, R.; Oh, S. H.; Lee, J.-H.; Yim, T.; Adams, B.; Nazar, L. F. *J. Am. Chem. Soc.* **2012**, *134*, 2902−2905.